Supplementary Materials for

Observation of anyonic Bloch oscillations

Weixuan Zhang[1*], Hao Yuan[1*], Haiteng Wang[1], Fengxiao Di[1], Na Sun[1], Xingen Zheng[1], Houjun Sun[2], and Xiangdong Zhang[1$]

[1]Key Laboratory of advanced optoelectronic quantum architecture and measurements of Ministry of Education, Beijing Key Laboratory of Nanophotonics & Ultrafine Optoelectronic Systems, School of Physics, Beijing Institute of Technology, 100081, Beijing, China

[2] Beijing Key Laboratory of Millimeter wave and Terahertz Techniques, School of Information and Electronics, Beijing Institute of Technology, Beijing 100081, China

*These authors contributed equally to this work. [$]Author to whom any correspondence should be addressed. E-mail: zhangxd@bit.edu.cn

S1. Details of the derivation of the eigen-equation for the 2D circuit simulator with $\theta = \pi$.

In this part, we give a detailed derivation of circuit eigen-equation, which could be mapped to the 1D stationary Schrödinger equation of two pseudofermions. Here, each lattice site possesses two circuit nodes. In this case, the voltage and current at the site (m, n) should be written as $V_{(m,n)}$

=$[V_{(m,n),1},\ V_{(m,n),2}]^T$ and $I_{(m,n)}$=$[I_{(m,n),1},\ I_{(m,n),2}]^T$. And, the voltage on the circuit node (m, n) is in the form of $V_{(m,n),j}e^{i\omega t}$ (j=1 and 2).

At first, we focus on the node pair located at the diagonal line (n, n). Carrying out the Kirchhoff's law on the circuit node pair (n, n), we get the following equation as:

$$\begin{vmatrix} I_{(n,n),1} \\ I_{(n,n),2} \end{vmatrix} = i\omega^{-1}\{-\frac{1}{L}\begin{vmatrix} 1 & -1 \\ -1 & 1 \end{vmatrix}\begin{vmatrix} V_{(n,n),1} \\ V_{(n,n),2} \end{vmatrix} + \omega^2 C \begin{vmatrix} V_{(n,n),1} - V_{(n-1,n),1} \\ V_{(n,n),2} - V_{(n-1,n),2} \end{vmatrix} + \omega^2 C \begin{vmatrix} V_{(n,n),1} - V_{(n+1,n),1} \\ V_{(n,n),2} - V_{(n+1,n),2} \end{vmatrix}$$

$$+\omega^2 C \begin{vmatrix} V_{(n,n),1} - V_{(n,n-1),2} \\ V_{(n,n),2} - V_{(n,n-1),1} \end{vmatrix} + \omega^2 C \begin{vmatrix} V_{(n,n),1} - V_{(n,n+1),2} \\ V_{(n,n),2} - V_{(n,n+1),1} \end{vmatrix}$$

$$+\omega^2 C_U \begin{vmatrix} V_{(n,n),1} \\ V_{(n,n),2} \end{vmatrix} + \omega^2 (n+n) C_F \begin{vmatrix} V_{(n,n),1} \\ V_{(n,n),2} \end{vmatrix} + \omega^2 C_e \begin{vmatrix} V_{(n,n),1} \\ V_{(n,n),2} \end{vmatrix}\}, \quad \text{(S1)}$$

where C_U, C_e and $(n+n)C_F$ are capacitances linking the node (n, n) to the ground. C is the capacitance used for connecting circuit nodes belonging to adjacent lattice sites. L is the inductor linking the circuit nodes belonging to the same lattice site.

We assume that there is no external source, so that the current flowing out of the node is zero. In this case, Eq. (S1) becomes:

$$\frac{1}{\omega^2 L}\begin{vmatrix} 1 & -1 \\ -1 & 1 \end{vmatrix}\begin{vmatrix} V_{(n,n),1} \\ V_{(n,n),2} \end{vmatrix} = [4C + C_U + C_e + (n+n)C_F]\begin{vmatrix} V_{(n,n),1} \\ V_{(n,n),2} \end{vmatrix}$$

$$-C\begin{bmatrix} 0 & 1 \\ 1 & 0 \end{bmatrix}(\begin{vmatrix} V_{(n,n-1),2} \\ V_{(n,n-1),1} \end{vmatrix} + \begin{vmatrix} V_{(n,n+1),2} \\ V_{(n,n+1),1} \end{vmatrix}) - C\begin{vmatrix} V_{(n-1,n),1} \\ V_{(n-1,n),2} \end{vmatrix} - C\begin{vmatrix} V_{(n+1,n),1} \\ V_{(n+1,n),2} \end{vmatrix}. \quad \text{(S2)}$$

Performing the diagonalization of Eq. (S2) with a unitary transformation:

$$F = \frac{1}{\sqrt{2}}\begin{bmatrix} 1 & e^{i\pi} \\ 1 & -e^{i\pi} \end{bmatrix}, \quad \text{(S3)}$$

Eq. (S2) becomes:

$$\frac{1}{\omega^2 L}\begin{vmatrix} 0 & 0 \\ 0 & 2 \end{vmatrix}\begin{vmatrix} V_{\uparrow,(n,n)} \\ V_{\downarrow,(n,n)} \end{vmatrix} = [4C + C_U + C_e + (n+n)C_F]\begin{vmatrix} V_{\uparrow,(n,n)} \\ V_{\downarrow,(n,n)} \end{vmatrix} - C\begin{bmatrix} 1 & 0 \\ 0 & e^{-i\pi} \end{bmatrix}\begin{vmatrix} V_{\uparrow,(n,n-1)} \\ V_{\downarrow,(n,n-1)} \end{vmatrix}$$

$$-C\begin{bmatrix} 1 & 0 \\ 0 & e^{i\pi} \end{bmatrix}\begin{vmatrix} V_{\uparrow,(n,n+1)} \\ V_{\downarrow,(n,n+1)} \end{vmatrix} - C\begin{vmatrix} V_{\uparrow,(n-1,n)} \\ V_{\downarrow,(n-1,n)} \end{vmatrix} - C\begin{vmatrix} V_{\uparrow,(n,n+1)} \\ V_{\downarrow,(n,n+1)} \end{vmatrix}\}. \quad \text{(S4)}$$

The new basis are $V_{\uparrow(\downarrow),(m,n)}=F[V_{(m,n),1},\ V_{(m,n),2}]^{\mathrm{T}}$, which are two decoupled terms acting as a pair of pseudospins $V_{\uparrow,(m,n)} = (V_{(m,n),1} + V_{(m,n),2})/\sqrt{2}$ and $V_{\downarrow,(m,n)} = (V_{(m,n),1} - V_{(m,n),2})/\sqrt{2}$. Thus, Eq. (S4) can be divided into two independent equations as:

$$0 = [4C + C_U + C_e + (n+n)C_F]V_{\uparrow,(n,n)} - C(V_{\uparrow,(n,n-1)} + V_{\uparrow,(n,n+1)} + V_{\uparrow,(n-1,n)} + V_{\uparrow,(n,n+1)}), \quad \text{(S5)}$$

$$\frac{1}{\omega^2 L/2}V_{\downarrow,(n,n)} = [4C + C_U + C_e + 2nC_F]V_{\downarrow,(n,n)} - C(e^{-i\pi}V_{\downarrow,(n,n-1)} + e^{i\pi}V_{\downarrow,(n,n+1)} + V_{\downarrow,(n-1,n)} + V_{\downarrow,(n,n+1)}). \quad \text{(S6)}$$

Based on similar derivations, we can write the eigen-equation at any circuit node (m, n). As for the case of n=m-1, we have,

$$\frac{1}{\omega^2 L/2}V_{\downarrow,(n,n-1)} = [4C + C_U + C_e + 2nC_F]V_{\downarrow,(n,n-1)} - C(V_{\downarrow,(n,n-2)} + e^{i\pi}V_{\downarrow,(n,n)} + V_{\downarrow,(n-1,n-1)} + V_{\downarrow,(n+1,n-1)}). \quad \text{(S7)}$$

As for the case of n=m+1, we have,

$$\frac{1}{\omega^2 L/2}V_{\downarrow,(n,n+1)} = [4C + C_U + C_e + 2nC_F]V_{\downarrow,(n,n+1)} - C(e^{-i\pi}V_{\downarrow,(n,n)} + V_{\downarrow,(n,n+2)} + V_{\downarrow,(n-1,n+1)} + V_{\downarrow,(n+1,n+1)}). \quad \text{(S8)}$$

As for the case of $|n-m| > 1$, we have,

$$\frac{1}{\omega^2 L/2}V_{\downarrow,(m,n)} = [4C + C_U + C_e + 2nC_F]V_{\downarrow,(m,n)} - C(V_{\downarrow,(m,n-1)} + V_{\downarrow,(m,n+1)} + V_{\downarrow,(m+1,n)} + V_{\downarrow,(m-1,n)}). \quad \text{(S9)}$$

Combing Eqs. (S6)-(S9), the eigen-equation of the designed circuit simulator is described by:

$$(f_0{}^2/f^2 - 4 - C_e/C)V_{\downarrow,mn} = -e^{-i\pi(\delta_{m,n}+\delta_{m,n+1})}V_{\downarrow,m(n+1)} - e^{i\pi(\delta_{m,n}+\delta_{m+1,n})}V_{\downarrow,m(n-1)}$$

$$-V_{\downarrow,(m+1)n} - V_{\downarrow,(m-1)n} + (C_U/C)V_{\downarrow,mn} + (m+n)(C_F/C)V_{\downarrow,mn}. \quad \text{(S10)}$$

We provide the following identification of tight-binding parameters in terms of circuit elements as:

$$J = 1, U = \frac{C_U}{C},\ F = \frac{C_F}{C}, \qquad \varepsilon = \frac{f_0{}^2}{f^2} - 4 - \frac{C_e}{C}, \qquad f_0 = \frac{1}{2\pi\sqrt{CL/2}}, \quad \text{(S11)}$$

where J, F, U and ε correspond to the strength of the particle hopping, external forcing, on-site interaction and the eigen-energy of two anyons. In this case, Eq. (S10) becomes:

$$\varepsilon c_{mn} = -J[e^{i\theta(\delta_{m,n}+\delta_{m+1,n})}c_{m(n-1)} + e^{-i\theta(\delta_{m,n}+\delta_{m-1,n})}c_{m(n+1)} + c_{(m-1)n} + c_{(m+1)n}]$$

$$+U\delta_{mn}c_{mn} + F(m+n)c_{mn} \quad \text{(S12)}$$

with c_{mn} corresponding to $V_{\downarrow,(m,n)}$. It is noted that Eq. (S12) is consistent with the eigen-equation of

c_{mn} for the 1D pseudofermions (Eq. (4) in the main text).

S2. The influence of the value of C_e on the correspondence between eigen-spectra of 2D circuit simulators and 1D two-anyon models.

It is known that the appearance of Bloch oscillations depends on the equally spaced eigen-spectrum of two bosons and two pseudofermions, and the periods are determined by the associated energy level spacings. While, due to the nonlinear relationship between the eigen-frequency of circuit simulator and the eigen-energy of two anyons $f = f_0/(\varepsilon + 4 + C_e/C)^{1/2}$, the distribution of eigen-spectrum for the circuit simulator should not be equally spaced.

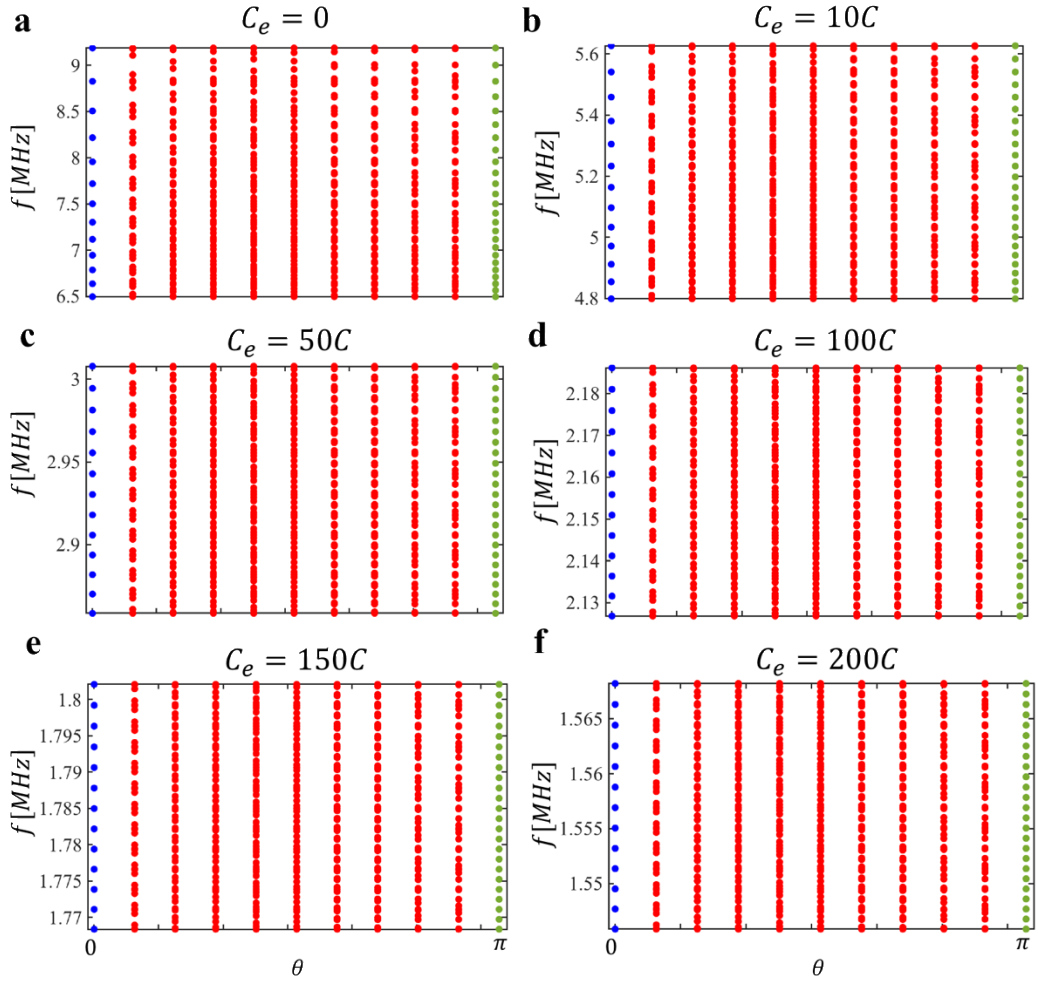

Fig. S1. (a)-(f) plot eigen-frequencies of designed circuit simulators as a function of the statistical angle

θ with $C_e = 0$, $C_e = 10C$, $C_e = 50C$, $C_e = 100C$, $C_e = 150C$, and $C_e = 200$C, respectively.

In this part, we show that such a deviation could become negligible with a large value of C_e used in our designed circuit. As shown in Figs. S1(a)-S1(f), we plot eigen-frequencies of designed circuit simulators as a function of the statistical angle θ with $C_e = 0$, $C_e = 10C$, $C_e = 50C$, $C_e = 100C$, $C_e = 150C$, and $C_e = 200$C, respectively. It is clearly shown that the eigen-spectrum with $C_e = 0$ is not equally spaced for the circuit simulator with $\theta = 0$ and $\theta = \pi$, where the frequency spacing is getting increased with the increase of eigen-frequencies. By increasing the value of C_e, the difference of frequency spacings belonging to the higher and lower eigen-frequencies ranges decreases. In our design, we set $C_e = 200C$. In this case, we can see that nearly equal-spaced eigen-spectra of circuit simulators with $\theta = 0$ ($\Delta f_B \approx 1862.57Hz$) and $\theta = \pi$ ($\Delta f_f \approx 931.28Hz$) appear. With such a good correspondence between the eigen-spectrum of designed 2D circuit and the 1D two-anyon model, the behavior of Bloch oscillation dominated by the quantum statistics can be effectively simulated by the designed circuit simulator.

S3. Numerical results of Bloch oscillations based on the 1D extended anyon-Hubbard model.

In this part, we give numerical results of BOs described by the 1D extended anyon-Hubbard model with *N*=23. The evolution equations for the probability amplitude c_{mn} can be obtained by substituting Eqs. (1) and (3) (in the main text) into the time-dependent Schrödinger equation $H|\psi>= i\frac{\partial}{\partial t}|\psi>$. In this case, we get

$$i\partial_t c_{mn} = -J[e^{i\theta(\delta_{m,n}+\delta_{m+1,n})}c_{m(n-1)} + e^{-i\theta(\delta_{m,n}+\delta_{m-1,n})}c_{m(n+1)}+c_{(m-1)n} + c_{(m+1)n}]$$

$$+U\delta_{mn}c_{mn} + F(m+n)c_{mn} \quad . \tag{S13}$$

To observe the BO of bosons and pseudofermions, the external excitation is set as:

$$c_{12,12}(t) = e^{i\varepsilon t} \quad . \tag{S14}$$

Here, other parameters are set as $\varepsilon = 20$, J=1, U=0 and F=0.5, respectively.

As shown in Figs. S2a and S2b, we calculate the evolution of $|c_{mn}(t)|^2$ with $\theta = 0$ and $\theta = \pi$, respectively. Moreover, Figs. S2c and S2d display the evolution of $|c_{12,12}(t)|$ with $\theta = 0$ and $\theta = \pi$, respectively. It is clearly shown that periodic breathing dynamics of both bosons and pseudofermions appear, and the oscillation period of the two bosons is almost twice of that of two pseudofermions.

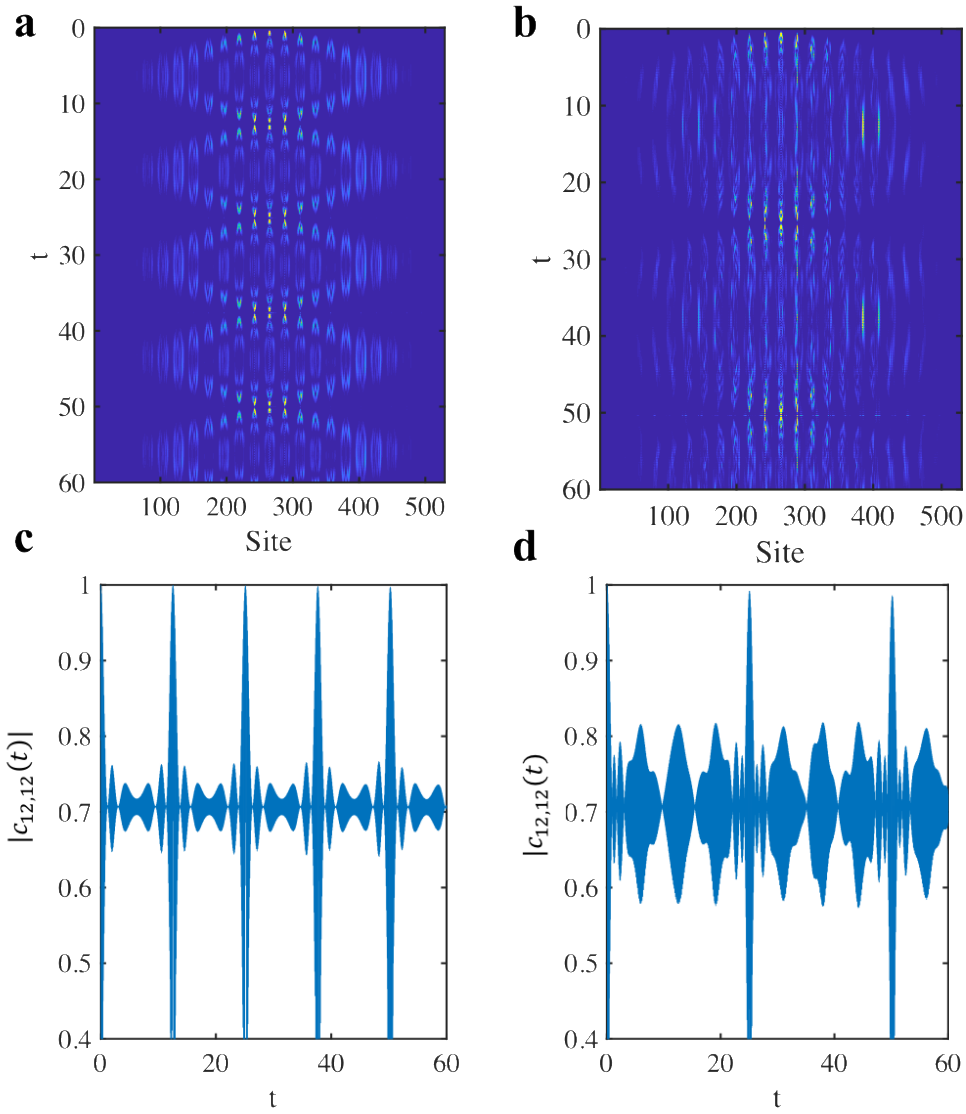

Fig. S2. (a) and (b) The evolution of $|c_{mn}(t)|^2$ with $\theta = 0$ and $\theta = \pi$ in the absence of particle

interactions, respectively. (c) and (d) display the evolution of $|c_{12,12}(t)|$ with $\theta = 0$ and $\theta = \pi$. Here, parameters are set as J=1, U=0 and F=0.5, respectively.

Then, we focus on the anyonic BOs with F=0.3. Figs. S3a and S3b present the calculated evolutions of $|c_{mn}(t)|^2$ with $\theta = 0$ and $\theta = \pi$, respectively. And, Figs. S3c and S3d display the associated evolution of $|c_{12,12}(t)|$ with $\theta = 0$ and $\theta = \pi$. It is clearly shown the larger the external force is, the larger the oscillation period and amplitude become. And, it is noted that the BO frequency related to a pair of pseudofermions ($\theta = \pi$) is always half of that for two bosons ($\theta = 0$).

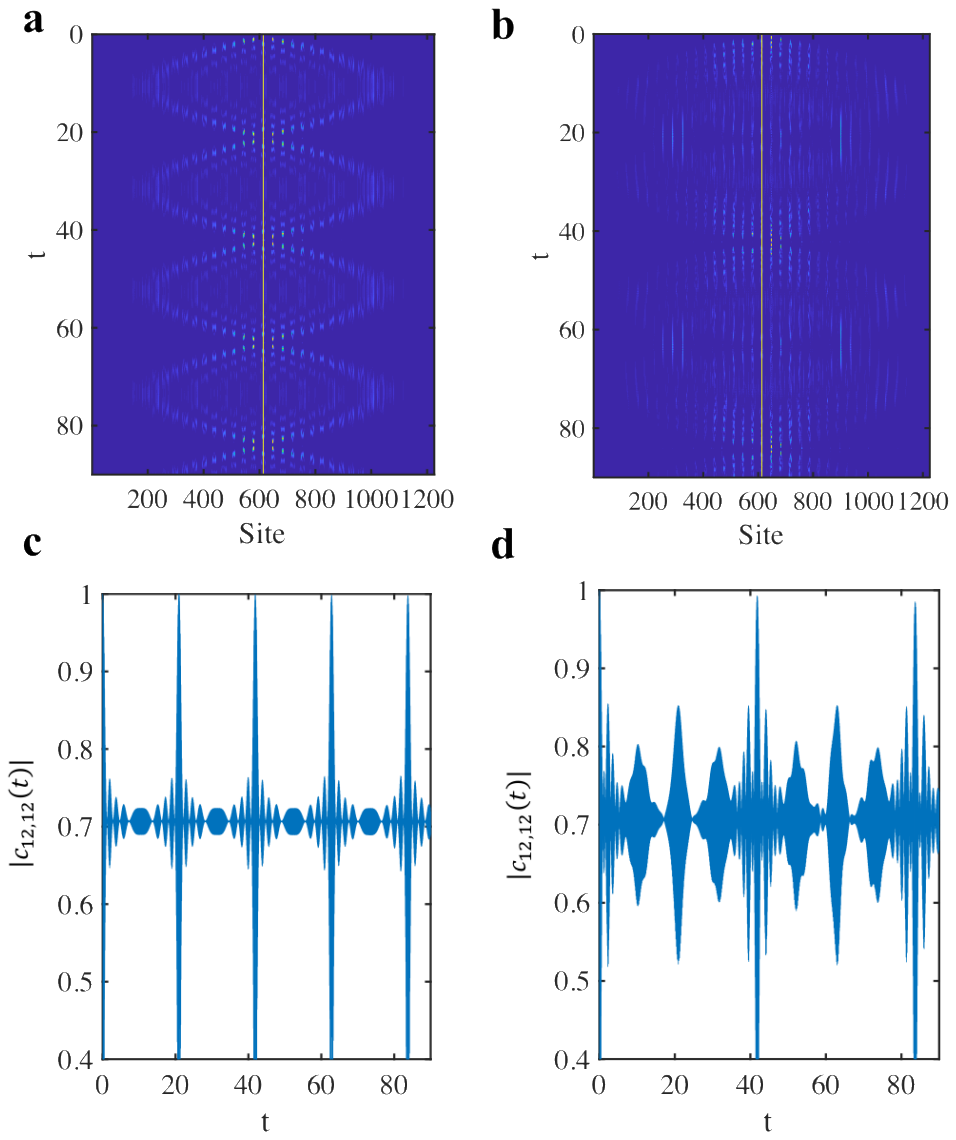

Fig. S3. (a) and (b) The evolution of $|c_{mn}(t)|^2$ with $\theta = 0$ and $\theta = \pi$ in the absence of particle

interactions, respectively. (c) and (d) display the evolution of the particle density function of $|c_{12,12}(\mathrm{t})|$ with $\theta = 0$ and $\theta = \pi$. Here, parameters are set as J=1, U=0 and F=0.3, respectively.

S4. Simulating the anyonic Bloch oscillation with different excitation frequencies, external forces and grounding capacitor C_e.

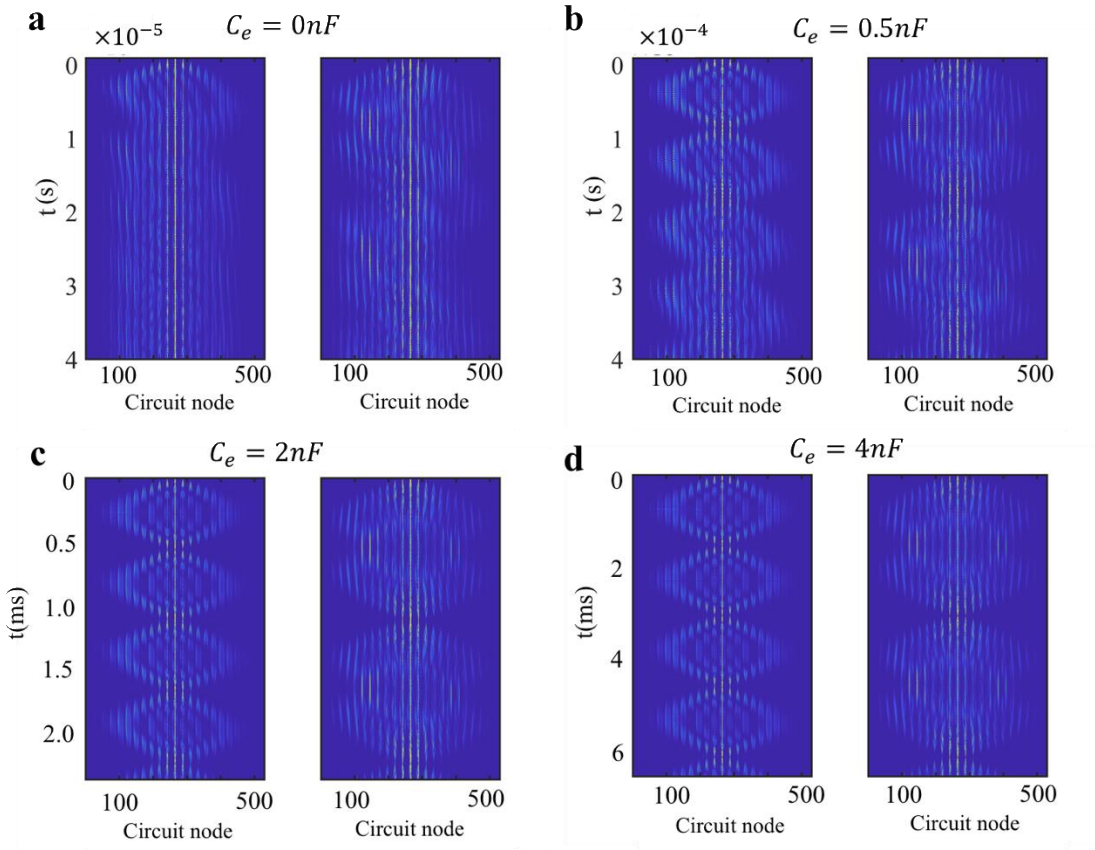

Fig. S4. (a)-(d) The time-dependent evolution of pseudospin $|V_{\downarrow,[m,n]}(t)|^2$ at each node in the circuit simulator with $C_e = 0$, $C_e = 0.5nF$, $C_e = 2nF$ and $C_e = 4nF$.

At first, we perform circuit simulations of BOs with different values of C_e. As shown in Figs. 4a-4d, we calculate the time-dependent evolution of pseudospin $|V_{\downarrow,[m,n]}(t)|^2$ at each node in the 2D circuit simulator (the left chart with $\theta = 0$ and the right chart with $\theta = \pi$) with $C_e = 0$, $C_e = 0.5nF$, $C_e = 2nF$ and $C_e = 4nF$, respectively, where the associated excitation frequencies are set as 9.19MHz,

3.01MHz, 1.56MHz, and 1.117MHz. Other parameters are the same to that used in Fig. 2. We can see that the larger the value of C_e is, the more ideal BOs appear. This is due to the fact that the nearly perfect eigen-spectrum with equal spacings could only be realized with an extremely large value of C_e, as shown in Fig. S1.

Then, we will simulate anyonic Bloch oscillations with a different external force by our designed electric circuits, that is $C_F = 3pF$. Before circuit simulations, we calculate the evolution of two-anyon eigen-energies as a function of θ with J=1 and F=0.3, as shown in Fig. S5a. And, the eigen-frequencies of designed circuit simulators with $C_e = 0$, $C_e = 50C$, and $C_e = 200$C are shown in Figs. S5(b)-S5(d). It is shown that the eigen-spectrum of the circuit simulator is consistent with that of two anyons with a large value of C_e. In particular, we have $\Delta f_B \approx 1130Hz$ and $\Delta f_f = 565Hz$. Next, we calculate the time-dependent evolution of pseudospin $|V_{\downarrow,[m,n]}(t)|^2$ at each node in the 2D circuit simulator ($C_e =$ 200C and $C_F = 0.3C$) with $\theta = 0$ and $\theta = \pi$, as shown in Fig. S6a and S6b. Here, the excitation frequency is set as 1.511MHz, and the voltage-pseudospin is excited by setting the input signal as $[V_{(12,12),1} = V_0, V_{(12,12),2} = -V_0]$ with $V_0 = 1V$. It is shown that the absolute value of pseudospin displays the periodic breathing dynamics for both conditions. Moreover, we note that the oscillation periods of bosonic circuits ($T_B \approx \frac{1}{\Delta f_B} = 0.885ms$) is nearly the half of the oscillation period for two pseudofermions ($T_f \approx \frac{1}{\Delta f_f} = 1.77ms$). Comparing to the results with $C_F = 0.5C$, we find that the smaller the external force is, the larger the oscillation period and amplitude become.

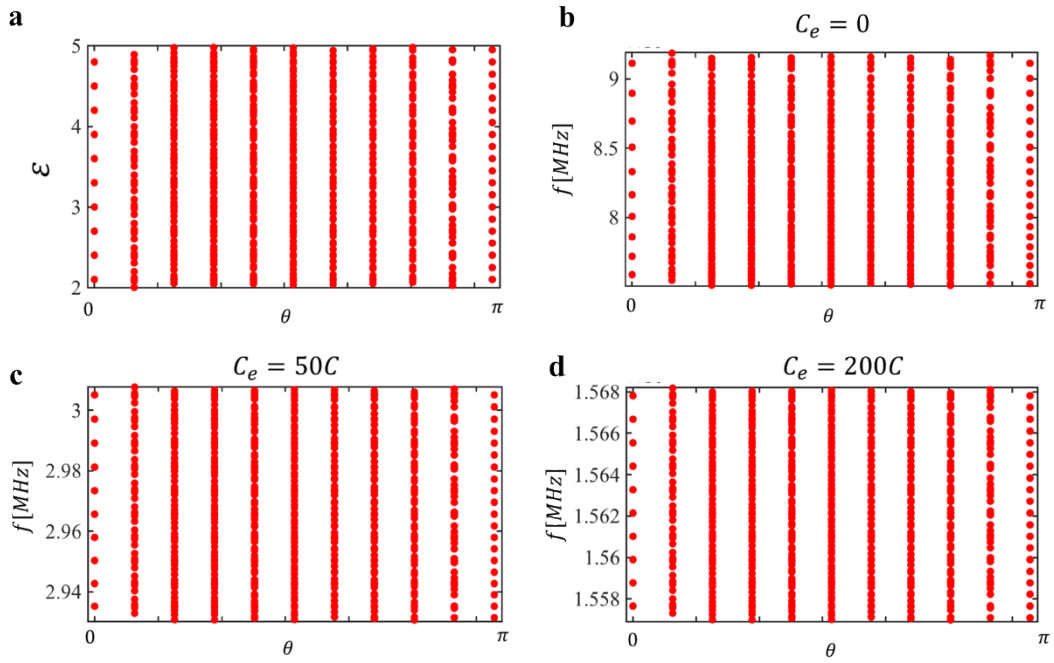

Fig. S5. (a). The evolution of two-anyon eigen-energies as a function of θ with J=1 and F=0.3. (b)-(d) The eigen-frequencies of circuit simulators ($C_F = 0.3C$) with $C_e = 0$, $C_e = 50C$, and $C_e = 200$C.

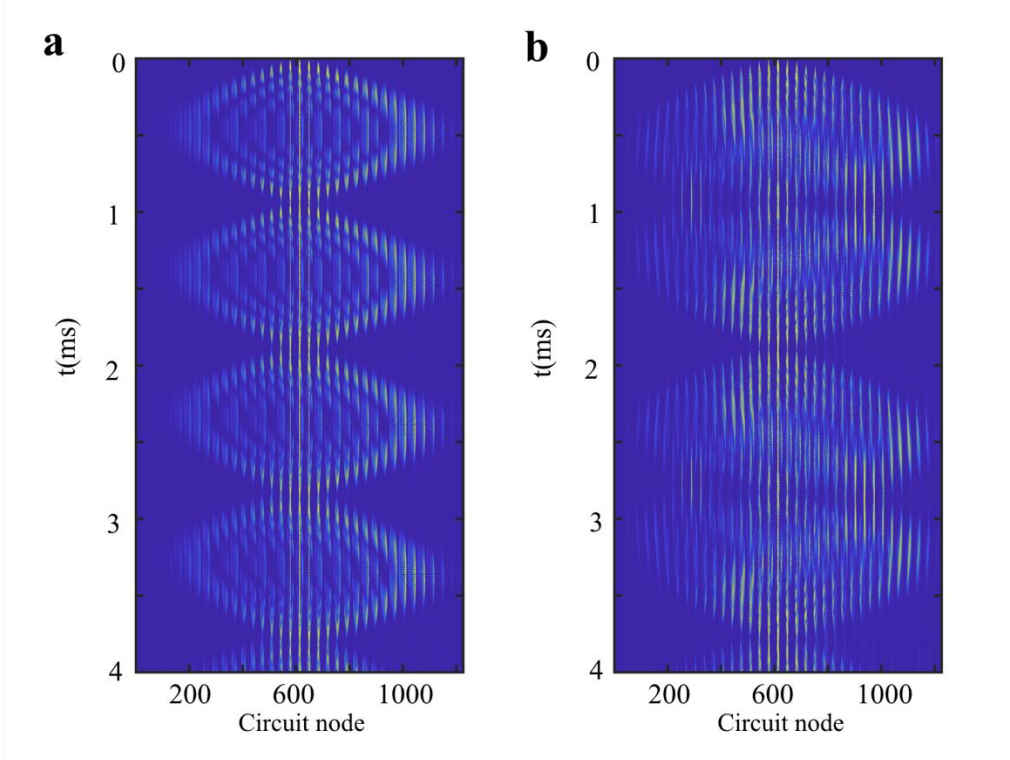

Fig. S6. The time-dependent evolution of pseudospin $|V_{\downarrow,[m,n]}(t)|^2$ at each node in the circuit simulator ($C_e = 200$C and $C_F = 0.3C$) with $\theta = 0$ for (a), and $\theta = \pi$ for (b).

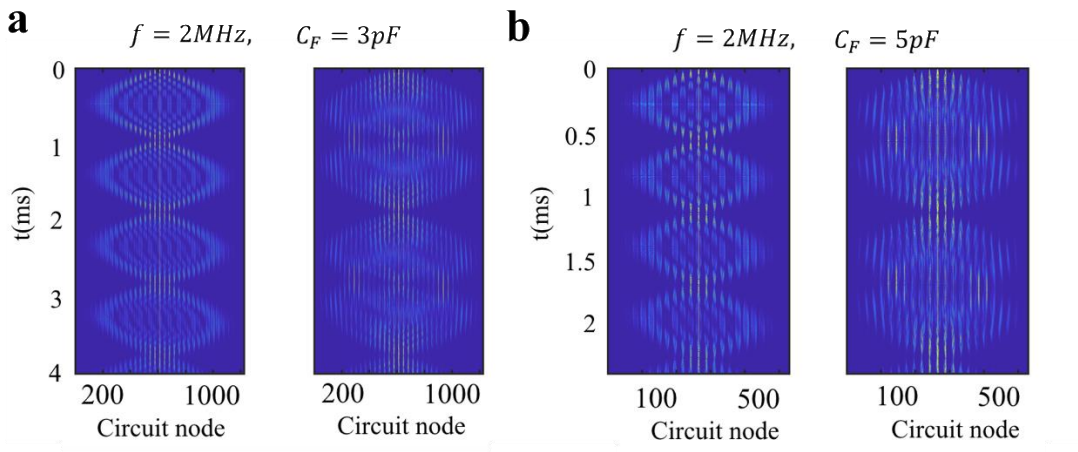

Fig. S7. The time-dependent evolution of pseudospin $|V_{\downarrow,[m,n]}(t)|^2$ at each node in the circuit simulator with $C_F = 0.3C$ for (a), and $C_F = 0.5C$ for (b). The associated excitation frequency is 2MHz.

At last, we perform circuit simulations of BOs under high excitation frequencies. The time-dependent evolution of pseudospin $|V_{\downarrow,[m,n]}(t)|^2$ at each node in the 2D circuit simulator with $C_F = 0.3C$ and $C_F = 0.5C$ are shown in Figs. S7a and S7b, where the associated excitation frequency is 2MHz. Other parameters are set as $C_e = 2nF$, $C = 10pF$, and $L = 10uH$. Comparing to the corresponding results with lower excitation frequencies (Fig. 2 for $C_F = 0.5C$ and Fig. S6 for $C_F = 0.3C$), we find that the more symmetric BO could be realized with a higher excitation frequency.

S5. The precise correspondence between time-dependent Schrödinger equation of two bosons and two pseudofermions and designed RC circuit simulators.

It is worthy to note that the stationary eigen-equation of our designed *LC* circuit is consistent with the stationary Schrödinger equation of the 1D anyon-Hubbard model with two anyons. As for the time-dependent evolution equation, the voltage of *LC* circuit follows second-order time differential, which is

different from the first-order time differential of quantum wave functions. In this part, we will design another kind of electric circuit based on resistances and capacitances to precisely match the time-dependent Schrödinger equation of two anyons with $\theta = 0$ and $\theta = \pi$.

The designed *RC* circuit simulator with $\theta = 0$ is plotted in Fig. S8a. Here, the associated 1D lattice length is *N*. We note that the designed circuit simulator contain $2N^2$ nodes, where the row (column) of N^2 nodes are labeled by *r*=(1, 1),…,(*N*, *N*) [*c*=(*N*+1,*N*+1),…,(2*N*, 2N)]. The voltages of totally N^2 circuit node in the top-row (left-column) correspond to the (copy of) probability amplitudes of two anyons with $\theta = 0$ in the 1D lattice of *N* sites. Specifically, the probability amplitude of two-boson states c_{mn} is mapped to the voltage signal on the circuit node (*m*, *n*) as $V_{m,n}$. Each node is connected to an external DC through a switch to apply an initial voltage signal. Two nodes (with one from the row and the other from the column) are connected by a suitably designed negative impedance converters with current inversion (INICs), named as R_{rc}, to realize the hopping, on-site interactions and external forcing. Specially, the designed INIDs for realizing the particle hoppling rate (R_{rc} =R_J) and the external force (R_{rc} =R_F/(m+n)) are enclosed by yellow and red blocks, respectively. Here, we set the on-site interaction as zero. As for the grounding, the green (blue) circuit node in the row (column) is grounded with a constant capacitor *C* and an INIC (normal resistor) with the effective resistance being R_{r0} (R_{c0}). In this case, the effective hoppling rate between node *r*=(*m*, *n*) and *c*=(m', n') is $J = \frac{1}{CR_J}$, where the node locations should satisfy the relation of $n' = n \pm 1 + N$ and $m' = m + N$ or $n' = n + N$ and $m' = m \pm 1 + N$. The external force could be mapped to the position-dependent grounding $R_F/(m + n)$ with *r*=(*m*,*n*) and c=(*m*+*N*,*n*+*N*). In this case, the effective external force is $F = \frac{1}{CR_F}$. The detailed node connections are plotted in the right-bottom part of Fig. S8a.

By switching off all switches at the same time (applying an initial state), the evolution of voltage

at each circuit node can be derived using the time-dependent Kirchhoff's equation as:

$$C\frac{dV_r}{dt}-\frac{V_r}{R_{r0}}=\sum_c\frac{V_c-V_r}{R_{rc}}\ ,$$

$$C\frac{dV_c}{dt}+\frac{V_c}{R_{c0}}=\sum_r\frac{V_r-V_c}{-R_{rc}} \tag{S15}$$

with $V_r\,(V_c)$ being the voltage at the circuit node in the row (column). The summation is limited to the connected circuit nodes. Defining the voltages at all circuit nodes as $|V(t)>=[V_{(1,1)}(t),\dots,V_{(N,N)}(t),V_{(N+1,N+1)}(t),\dots,V_{(2N,2N)}(t)]$, Eq. (S15) could be expressed in the matrix form as $i\partial_t|V(t)>=\Xi|V(t)>$, where the off-diagonal components of circuit Hamiltonian Ξ are $\Xi_{rc}=i\frac{1}{CR_{rc}}$ and $\Xi_{cr}=-i\frac{1}{CR_{rc}}$, and the diagonal components are given by $\Xi_{rr}=i\frac{1}{C}(\frac{1}{R_{r0}}-\sum_c\frac{1}{R_{rc}})$ and $\Xi_{cc}=i\frac{1}{C}(-\frac{1}{R_{c0}}+\sum_r\frac{1}{R_{rc}})$. By appropriately setting the grounding INICs as $\frac{1}{R_{r0(i)}}=\sum_k\frac{1}{R_{ik}}$ and the grounding resistances as $\frac{1}{R_{c0(i)}}=\sum_k\frac{1}{R_{ik}}$, the circuit Hamiltonian can be expressed as:

$$\Xi=i\begin{vmatrix}0 & -\Pi\\ \Pi & 0\end{vmatrix} \tag{S16}$$

with Π being a $N\times N$ matrix. In this case, when the nodes connecting and grounding resistances are suitably applied, the form of $N\times N$ matrix Π can be the same to the Hamiltonian of the 1D two-boson model. In this case, the voltage evolution in the designed RC circuit could be the same to the probability amplitude of two bosons.

Based on the similar method, the RC circuit related to two pseudofermions $\theta=\pi$ could also be designed. Fig. S8b shows the corresponding connection pattern at different circuit nodes. Comparing to the circuit for two bosons, the only difference is that there are a few of effective hopping rates sustaining a phase $e^{i\pi}$. This could be easily fulfilled by reversing the biased voltage of the associated grounding and connecting INICs.

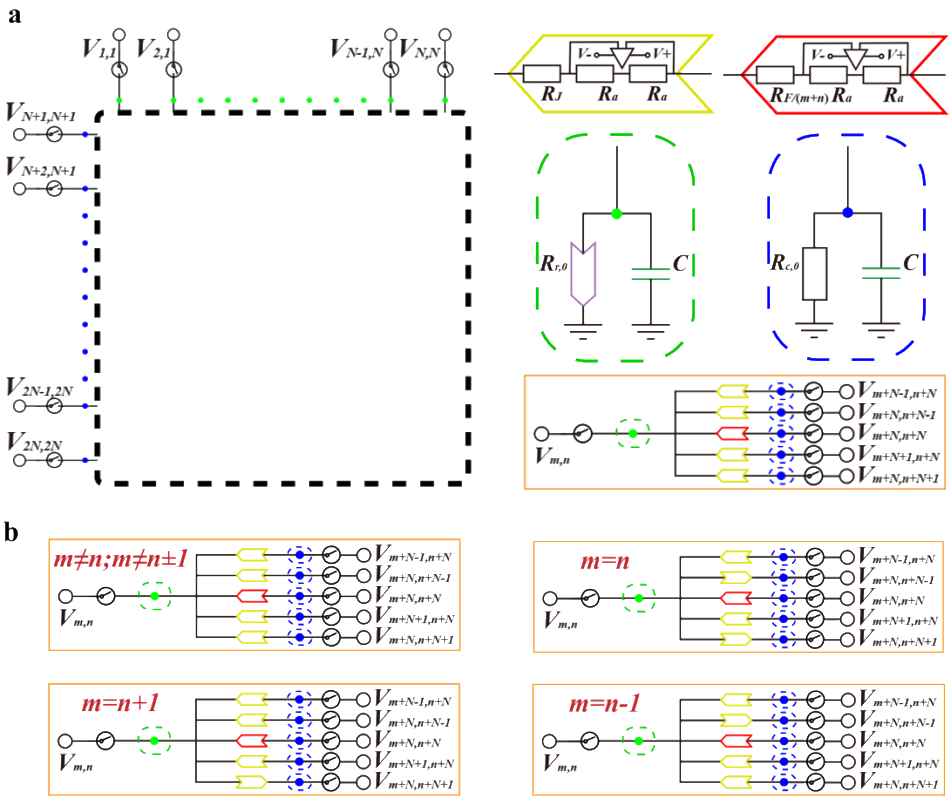

Fig. S8. (a) and (b) The designed *RC* circuit for simulating Bloch oscillations of two bosons and two pseudofermions.

Then, we use the designed *RC* circuit to simulate the BOs of two bosons and two pseudofermions. Other parameters are set as *N*=35, *C*=*1*uF, $R_J = 1000\Omega$, $R_F = 2000\Omega$ and $R_a = 100\Omega$. And, the initial voltage distribution is set as: $V_{mn}(t=0) = V_0\delta_{12,12}$. As shown in Fig. S9a and S9b, we present the calculated evolution of the signal $|V_{\downarrow,[m,n]}(t)|^2$ in the circuit simulators for two bosons and two pseudofermions, respectively. And, the corresponding time-dependent evolutions of $|V_{\downarrow,[12,12]}|^2$ are presented in Figs. S9c and S9d.

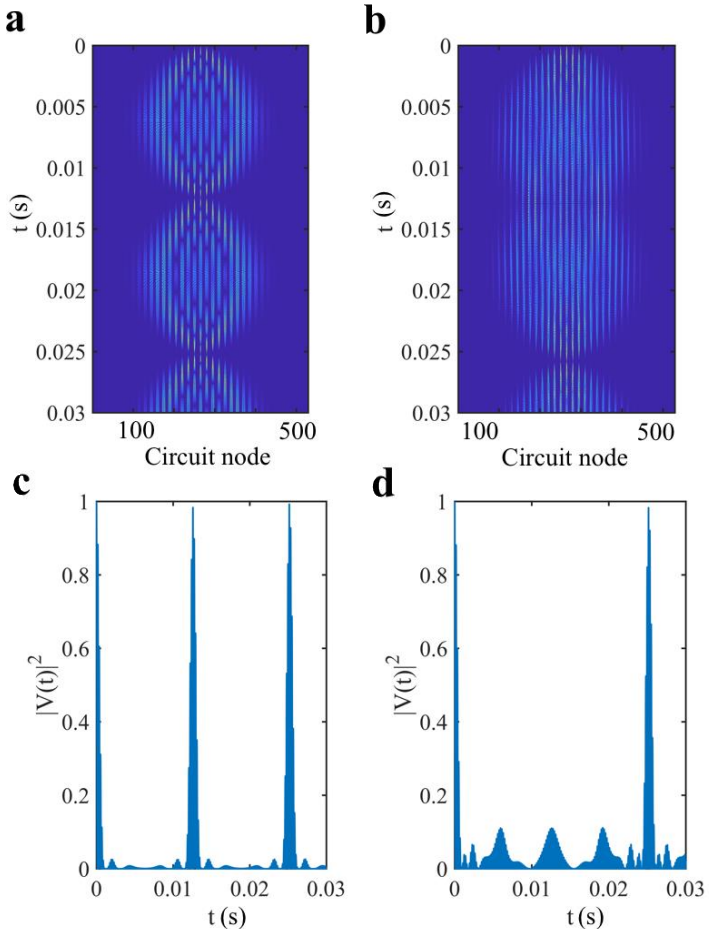

Fig. S9. (a) and (b) The evolution of the signal $|V_{\downarrow,[m,n]}(t)|^2$ in the circuit simulators for two bosons and two pseudofermions, respectively. (c) and (d) The time-dependent evolutions of $|V_{\downarrow,[12,12]}|^2$ for two bosons and two pseudofermions.

For comparison, we also calculate the evolution of $|c_{mn}(t)|^2$ of two bosons and two pseudofermions in the 1D anyon-Hubbard model, as shown in Figs. S10a and S10b. The associated parameters are set as J=1, F=0.5 and $C_{mn}(t=0)=\delta_{12,12}$. And, the corresponding time-dependent evolutions of $|c_{12,12}|^2$ are presented in Figs. S10c and S10d. We note that a good agreement for the time-dependent evolution of voltages and probability amplitude is obtained. In particular, it is clearly shown that the oscillation period in the two-boson simulator is twice of that in the two-pseudofermion

simulator, that is consistent with the theoretical prediction.

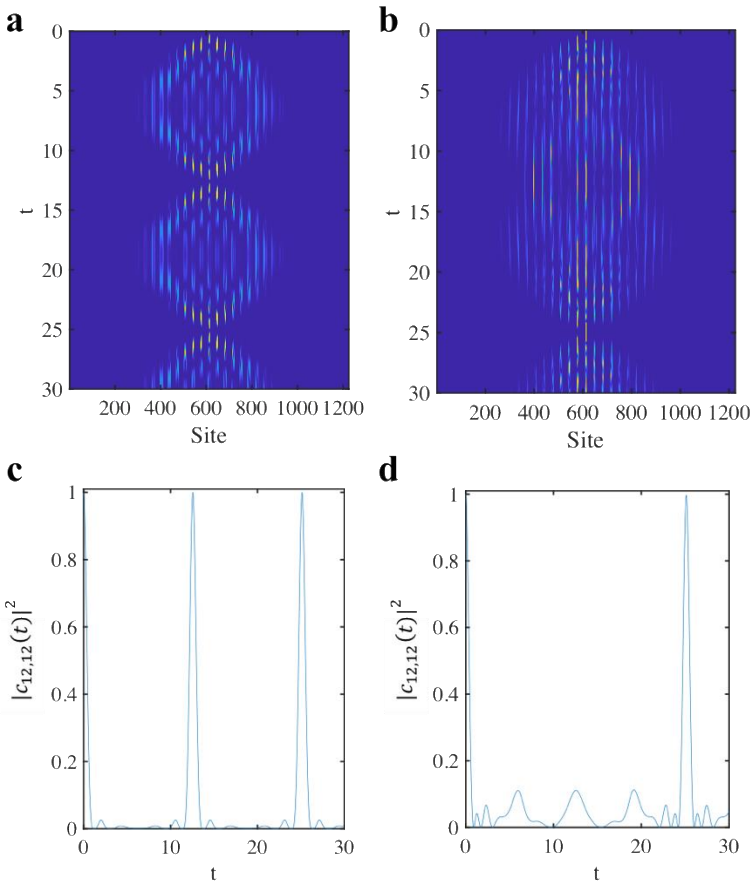

Fig. S10. (a) and (b) The evolution of $|c_{mn}(t)|^2$ for two bosons and two pseudofermions in the 1D anyon-Hubbard model. (c) and (d) The time-dependent evolutions of $|c_{12,12}|^2$ for two bosons and two pseudofermions.